

the energy loss at  $\hbar\omega_p$ , due to excitation of the void breathing mode should gradually broaden as a result of the smearing out of the breathing-mode density of states. Such broadening could be observable for aluminum, where the unperturbed plasmon energy is fairly sharp. Unfortunately, the plasmon structure of bulk transition metals where the void arrays have been produced is already so ill defined that it might be difficult to detect even the few-eV

broadening of the spectrum, which would correspond to the bandwidth of the breathing mode.

#### ACKNOWLEDGMENTS

The author wishes to thank Dr. M. Anderegg for helpful comments and discussions on this subject. He also expresses his gratitude to Dr. E. A. Trendelenburg, Dr. B. Fitton, and the staff of the Surface Physics Division of ESTEC for their hospitality.

\* Chercheur Qualifié au Fonds National Belge de la Recherche Scientifique.

<sup>1</sup>C. Cawthorne and E. J. Fulton, *Nature* **216**, 576 (1967).

<sup>2</sup>J. H. Evans, *Nature* **229**, 403 (1971); G. I. Kulcinski, J. L. Brimhall, and H. E. Kissinger, *J. Nucl. Mater.* **40**, 166 (1971).

<sup>3</sup>J. H. Evans, *Radiation Effects* **10**, 55 (1971).

<sup>4</sup>J. Schmit and A. A. Lucas, *Solid State Comm.* **11**, 415 (1972); **11**, 419 (1972).

<sup>5</sup>V. Peuckert, *Z. Physik* **241**, 191 (1971); R. A. Craig, *Phys. Rev.* (to be published).

<sup>6</sup>N. G. van Kampen, B. R. A. Nijboer, and K. Schram, *Phys. Letters* **26A**, 307 (1968).

<sup>7</sup>J. Th. G. Overbeek, *Discussions Faraday Soc.* **42**, 7 (1966).

<sup>8</sup>K. Malén and R. Bullough, in *British Nuclear Engineering Conference, Reading*, 1971, edited by S. F. Piegh, M. H. Loreto, and D. I. R. Morris.

<sup>9</sup>A. M. Stoneham, *J. Phys. F. Metal Phys.* **1**, 778 (1971).

<sup>10</sup>V. K. Tewary and R. Bullough, Atomic Energy Research Establishment Harwell Technical Report No. TP 479 (unpublished).

<sup>11</sup>R. Englman and R. Ruppin, *J. Phys. C* **1**, 614 (1968); *Rep. Progr. Phys.* **33**, 149 (1970).

<sup>12</sup>E. N. Economou, *Phys. Rev.* **182**, 539 (1969).

<sup>13</sup>C. Kittel, *Introduction to Solid State Physics* (Wiley,

New York, 1971).

<sup>14</sup>A. A. Lucas and M. Sunjić, *Progr. Surface Sci.* **2**, 75 (1972).

<sup>15</sup>J. D. Jackson, *Classical Electrodynamics* (Wiley, New York, 1962), p. 115.

<sup>16</sup>M. Natta, *J. Phys. (Paris)* **31**, C1-53 (1970); P. Henoc and L. Henry, *J. Phys. (Paris)* **31**, C1-55 (1970).

<sup>17</sup>D. V. Paranjape and W. J. Heaney, *Phys. Rev. B* **6**, 1743 (1972).

<sup>18</sup>S. Raimes, *The Wave Mechanics of Electrons in Metals* (North-Holland, Amsterdam, 1967), p. 283. Raimes uses a similar argument to derive the bulk plasma frequency in a solid metallic medium. For this case, one must assume that the electron gas is compressible to accommodate the inward current. For surface plasmons, on the contrary, the electron gas acts as if it was incompressible so that only superficial charge density fluctuations occur and a cavity is required. For a solid sphere, bulk radial electron compression waves exist but their field is zero outside the sphere.

<sup>19</sup>D. Polder and H. Casimir, *Phys. Rev.* **73**, 360 (1948); M. R. Aub and S. Zienau, *Proc. Roy. Soc. A* **257**, 464 (1964); A. D. McLachlan, *Mol. Phys.* **6**, 423 (1963).

<sup>20</sup>S. Lundqvist and A. Sjölander, *Arkiv Fysik* **26**, 17 (1964).

<sup>21</sup>A. A. Lucas, *Physica* **35**, 353 (1967).

<sup>22</sup>R. Castaing and L. Henry, *C. R. Acad. Sciences Paris* **255**, 76 (1962).

### Optical Properties of Single-Crystal Be from 0.12 to 4.5 eV

J. H. Weaver, D. W. Lynch, and R. Rosei\*

Ames Laboratory-USAEC and Department of Physics, Iowa State University, Ames, Iowa 50010

(Received 11 October 1972)

Measurements of the optical absorptivity of single crystals of Be have been carried out in the energy range 0.12–4.5 eV with polarized light. The infrared absorptivity is considerably lower than previously reported. Evidence is presented for the onset of interband transitions for both polarizations beginning near 0.4 eV. A shoulder is noted in the absorptivity for ELc at about 1.3 eV. The absorptivity data are Kramers-Kronig analyzed and the optical constants are determined. An interpretation based on the band structure of Tripp, Everett, Gordon, and Stark is presented.

#### INTRODUCTION

The optical properties of beryllium have been the subject of a number of experimental studies.<sup>1-9</sup>

Early workers studied Be films but either performed the evaporation in poor vacua or exposed the samples to contaminating atmospheres before or during the measurements. Tungsten contamina-

tion was suspected in at least one case. More recently, the optical constants have been measured at 82 and 290 K from 0.11 to 1.5 eV by Shklyarevskii and Yarovaya,<sup>6</sup> and in the vacuum ultraviolet from 10.5 to 26 eV by Toots, Fowler, and Marton.<sup>7</sup> Swanson determined the line shape of the characteristic electron-energy-loss peak of Be; LaVilla and Mendlowitz<sup>9</sup> subsequently Kramers-Kronig-analyzed Swanson's data to obtain the optical constants and the reflectivity in the 12–28-eV range. A comparison of the reflectivities of Toots, Fowler, and Marton and of LaVilla and Mendlowitz shows reasonable agreement. Thus, while infrared and vacuum uv data were available, no reliable optical measurements existed in the 1.5–10.5-eV range prior to this study. Further, without exception, the existing data were obtained with films rather than single crystals; no optical data existed to show the anisotropy for  $\vec{E} \parallel \hat{c}$  and  $\vec{E} \perp \hat{c}$ .

Band structures for Be have been calculated by Herring and Hill<sup>10</sup> [orthogonalized plane wave (OPW)], Cornwell<sup>11</sup> (local pseudopotential), Loucks and Cutler<sup>12</sup> (OPW), Terrell<sup>13</sup> [augmented plane wave (APW)], and Tripp *et al.*<sup>14</sup> (local and nonlocal pseudopotential). The resultant bands are in general agreement, but the Fermi surface given by the local-pseudopotential model was poor and a nonlocal model was needed to describe the Fermi surface accurately. A comparison of nonlocal and local pseudopotentials was carried out for Mg by Kimball *et al.*<sup>15</sup>; the two models gave nearly identical Fermi surfaces. The poor result for Be with the local model was discussed by Terrell,<sup>13</sup> who showed that the lack of *p*-like core states in Be makes the cancellation theorem invalid for *p*-like conduction states, while it should be operative for *s*-like conduction states. It has been shown<sup>16</sup> that if a local-pseudopotential model is valid, with only a few Fourier coefficients  $V_G$  of the pseudopotential, the optical conductivity will consist of edges at photon energies of  $2|V_G|$  with decaying tails toward higher energies. Such behavior has been observed in Al.<sup>17,18</sup> The local-pseudopotential coefficients of Tripp *et al.*<sup>14</sup> predict edges at 1.56 and 2.67 eV ( $\vec{E} \perp \hat{c}$ ) and 2.42 and 2.67 eV ( $\vec{E} \parallel \hat{c}$ ). Such edges were not observed, as was expected since the same model gave poor Fermi-surface results. In the nonlocal model, the parallel bands giving rise to the absorption edges exist only below the Fermi level and do not cross it at many places in  $\vec{k}$  space. We reproduce the bands of Tripp *et al.* and base our interpretation on them. To date, there have been no calculations of the interband conductivity  $\epsilon_2/\lambda$ , corresponding to those of Kasowski<sup>19</sup> for Zn and Cd. These would be most useful, of course, when comparing optical constants with theory.

In this paper we present the measured absorptiv-

ity of oriented single crystals of hcp beryllium. Our data extend from 0.12 to 4.5 eV and show very clearly the characteristics for  $\vec{E} \parallel \hat{c}$  and  $\vec{E} \perp \hat{c}$ , where  $\vec{E}$  is the electric field vector of the incident radiation.

## RESULTS AND DISCUSSION

Absorptivity measurements were carried out using a calorimetric technique which has been described elsewhere.<sup>20</sup> The data were obtained at 4.2 K and a 15° angle of incidence. Single crystals of Be were spark cut so that the  $\hat{c}$  axis was in the face; by using polarized radiation we were able to measure the absorptivity for both  $\vec{E} \parallel \hat{c}$  and  $\vec{E} \perp \hat{c}$ , thus providing identical sample treatment for both polarizations. The dimensions of the samples were about 8×12 mm.

Since Be is highly toxic, considerable care was taken when preparing the sample. Mechanical polishing was performed while the sample was immersed in glycerin. By using progressively finer abrasives, an excellent mirrorlike surface was obtained. To remove the work-damaged layer, an electropolishing technique<sup>21</sup> was used. The sample was electropolished for about 90 sec in a vigorously stirred solution of perchloric acid, ethyl alcohol, and butylcellosolve (20 : 70 : 10 by volume at about 0 °C). The sample was then washed in boiling alcohol, dried in a nitrogen stream, and mounted in the calorimeter sample chamber. An estimated 15 min elapsed during the mounting process and before the chamber was at 10<sup>-4</sup> Torr. Within 1 h the cooling to 77 K was initiated. While the effects of atmospheric contamination are significant in the vacuum ultraviolet, we believe that, since the band gap of BeO is about 10.5 eV,<sup>22</sup> the effects should be less important below 4.5 eV. Nevertheless, attempts have been

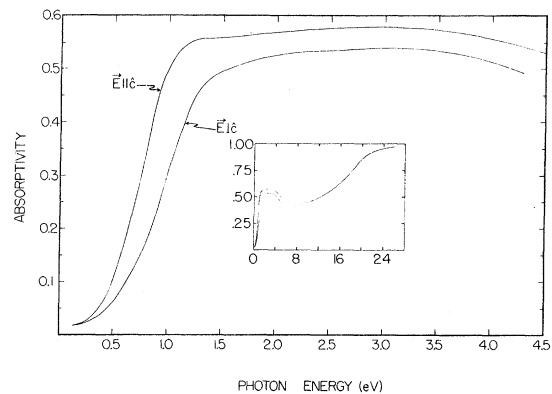


FIG. 1. Absorptivity of Be at 4.2 K, 15° angle of incidence. The insert shows smooth interpolations joining our results to those of Ref. 7. The interpolations were used only for KK analysis, and should not be taken seriously.

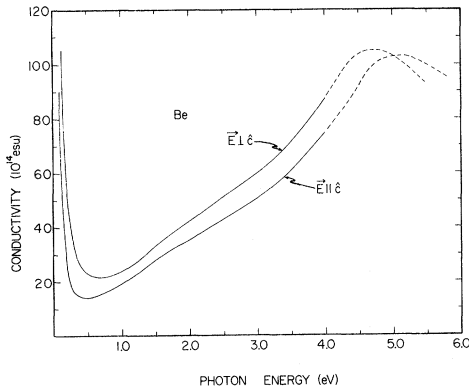


FIG. 2. Optical conductivity for Be. Above 4 eV, the magnitudes are not reliable, owing to the interpolation from 4.5 to 10.5 eV. The peaks persist for all interpolations used.

made to minimize the exposure of the sample.

Residual-resistivity-ratio measurements were performed to determine the anisotropy in the resistivity. It was found that for  $\vec{E} \parallel \hat{c}$   $\rho_{300}/\rho_{4.2}$  was 41.6, while for  $\vec{E} \perp \hat{c}$  it was 56.2. (Reference 14 reported a value of approximately 1000.) Published results on single crystals of Be by Grüneisen and co-workers<sup>23</sup> indicated that at 273 K,  $\rho_{\parallel} = 3.58$  and  $\rho_{\perp} = 3.12 \mu\Omega \text{ cm}$ , which gave  $(\rho_{\perp}/\rho_{\parallel})_{273} = 0.88$ , while at 4.2 K we found the ratio to be 0.65.

The absorptivity of Be is shown in Fig. 1. The high-energy limit is 4.5 eV for  $\vec{E} \parallel \hat{c}$  and 4.3 eV for  $\vec{E} \perp \hat{c}$ . The absorptivities rise sharply from about 0.2 eV, the  $\vec{E} \parallel \hat{c}$  rise being the more precipitous. Even in the range 0.12–0.20 eV, both curves display a steady rise. At 0.9 eV the difference  $A_{\parallel} - A_{\perp}$  is nearly 21%. For  $\vec{E} \parallel \hat{c}$ ,  $A$  levels off at 1.3 eV, but begins to rise again at 1.5 eV. This shoulder has no counterpart in  $\vec{E} \perp \hat{c}$ , which rises continuously to a maximum at 3.0 eV. Above 3.0 eV, the absorptivities drop off gradually.

Despite the relatively poor residual-resistivity ratios for our samples, at 4.2 K and 0.12 eV  $\omega\tau \approx 42$  and 35.5 for  $\vec{E} \parallel \hat{c}$  and  $\vec{E} \perp \hat{c}$ , respectively, as calculated using the dc values of the resistivity given in Ref. 23. The free-electron absorptivities are then 0.00031 and 0.00037, independent of frequency. The positive slope of the curves of Fig. 1 can then be attributed to interband absorption rather than a small value of  $\omega\tau$ , which would also cause  $A$  to rise as  $\omega$  increases. If the absorptivity at 0.12 eV is taken to be 0.019, it is clear that interband effects and the anomalous-skin-effect<sup>24,25</sup> corrections to the free-electron term are important.

The insert of Fig. 1 shows our data and the data of Toots, Fowler, and Marton<sup>7</sup> (obtained at a 20°

angle of incidence). To Kramers–Kronig analyze the data and obtain the optical constants, it was necessary to know the absorptivity between 4.5 and 10.5 eV. The dashed lines represent smooth structureless interpolations which were used for Kramers–Kronig (KK) analysis only; they should not be taken seriously. We have found that the principal change which results from altering the interpolation is an adjustment in the height of the conductivity peaks which appear at about 5.0 eV for both polarizations, as well as a shift in the magnitude of the optical constants at higher energy. No appreciable effect was noted in  $\vec{\epsilon}$  below 4.0 eV, and we consider our results to be reliable below this energy. Reliable information at higher energies must await further experimental work.

The optical conductivity is shown for both polarizations in Fig. 2. Both curves drop from large, free-electron values before turning up at about 0.5 and 0.7 eV for  $\vec{E} \parallel \hat{c}$  and  $\vec{E} \perp \hat{c}$ , respectively. While the rise in the conductivity does herald interband effects, it is not reasonable to say that such effects do not exist at lower energies. In fact, from the slope of the absorptivity curves, we must say that such effects do play a significant part in the absorption process at energies as low as 0.12 eV. It should be noted that the influence of the interpolation is beginning to be felt at about 4 eV and that the magnitude of the conductivity should not be taken seriously above 4 eV. This is indicated by dashed lines in Fig. 2. Since an altering of the interpolation does not change the position of the peak which persists for all interpolations used, we continue the spectra to 6 eV, noting that  $\vec{E} \parallel \hat{c}$  peaks at 5.1 and  $\vec{E} \perp \hat{c}$  peaks at 4.7 eV.

The real and imaginary parts of the dielectric function are shown in Fig. 3. For  $\vec{E} \parallel \hat{c}$ , a slight bump occurs in  $\epsilon_2$  at 1.6 eV, corresponding to the shoulder in the absorptivity at about 1.3 eV. The  $\epsilon_2$  curves reach “minima” at about 2.9 and 3.1 eV for  $\vec{E} \parallel \hat{c}$  and  $\vec{E} \perp \hat{c}$ , respectively. The real part of

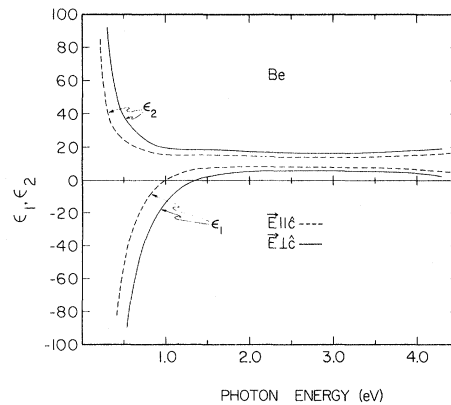


FIG. 3. Dielectric function for Be.

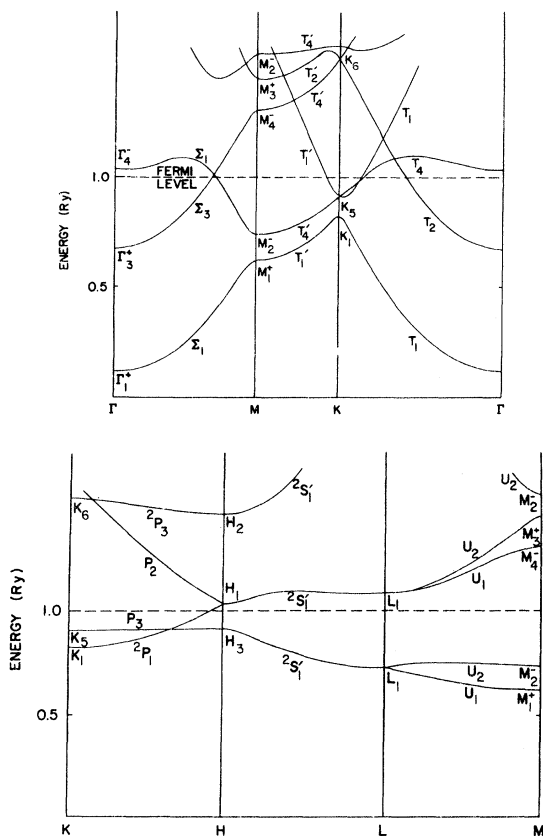


FIG. 4. Band structure for Be from Ref. 14.

$\tilde{\epsilon}$  rises from large negative values, passes through zero at 1.0 ( $\vec{E} \parallel \hat{c}$ ) and 1.36 eV ( $\vec{E} \perp \hat{c}$ ), with broad maxima at about 2.2 and 2.4 eV.

The band structures of Tripp, Everett, Gordon, and Stark<sup>14</sup> are reproduced in Fig. 4. A glance at this figure shows that the only filled bands which are parallel or nearly parallel and which cross the Fermi level are separated by at least 7 eV ( $\Sigma_1 - \Sigma_3$  and  $T_1 - T_2$ ); so we expect no parallel-band absorption (which was important in Al) in our data. There are no flat bands as in the noble metals, and few critical points separated by low energies. We thus expect that the dielectric constants will be rather devoid of structure. Of interest are the bands near  $H_1$  and  $H_3$ ,  $\Gamma_3^+$  and  $\Gamma_4^+$ , and  $L_1$ , the crossing of  $T_1$  and  $T_4$ , and the position of the Fermi energy. Interband transitions are possible near these symmetry points and, from the band scheme, they would be expected to occur at energies below about 5 eV. The strength of the transitions would be determined by the joint density of

states with selection rules forbidding certain transitions. Specifically, the transitions  $H_1 \rightarrow H_3$  and  $L_1 \rightarrow L_1$  are allowed for  $\vec{E} \perp \hat{c}$ , and  $\Gamma_3^+ \rightarrow \Gamma_4^+$  and  $L_1 \rightarrow L_1$  are allowed for  $\vec{E} \parallel \hat{c}$ .<sup>26</sup> Only the  $L_1 \rightarrow L_1$  transition seems to have an appreciable volume of nearby  $k$  space contributing to absorption near it. We might then expect an anisotropy to appear in the dielectric constants, with  $\vec{E} \perp \hat{c}$  displaying low-energy features corresponding to  $H_1 \rightarrow H_3$  [ $E(H_1) - E(H_3) \approx 1.6$  eV]. This anisotropy has not been observed. Indeed, while  $\vec{E} \parallel \hat{c}$  shows slight structure in  $\epsilon_2$  near 1.6 eV,  $\vec{E} \perp \hat{c}$  is featureless; the absorptivity of  $\vec{E} \parallel \hat{c}$  has a shoulder at 1.3 eV, while  $\vec{E} \perp \hat{c}$  is smooth. From Fig. 2, the similarity in the conductivities is apparent,  $\vec{E} \perp \hat{c}$  having the larger magnitude. Both show a minimum below 0.8 eV and a kink near 1.6 eV. It is apparent, then, that while  $H_1 \rightarrow H_3$  transitions may be playing a part in absorption between about 1 and 2 eV, other transitions are also important. Since the features are broad and washed out, it is possible that weaker effects may be entering in, e.g.,  $T_2 \rightarrow T_4$  for  $\vec{E} \parallel \hat{c}$ . It is not possible to say with conviction that our data confirm any features of the band structure. A calculation of the conductivity is required to determine the contributions of different transitions to the absorption processes.

In Fig. 2, we have speculated about structure near 5 eV. This can probably be associated with the points  $L$  and  $\Gamma$ .  $L_1 \rightarrow L_1$  transitions are allowed for both polarizations;  $E(L_1) - E(L_1) \approx 4.8$  eV. Near  $L$  the bands are seen to be nearly parallel over a considerable region of  $\vec{k}$  space and the resulting absorption would be strong. Transitions from  $\Gamma$  would also contribute to absorption for  $\vec{E} \parallel \hat{c}$  near 5 eV. It must again be stress that the height of the conductivity peaks is dependent upon the choice of interpolation. It seems unwise to do more than note that theory predicts structure near 5 eV and that a smooth interpolation from 4.5 to 10.5 eV produces it.

The partial sum rule giving  $N_{\text{eff}}(E)$ , the number of electrons per atom contributing to absorption below energy  $E$ , was calculated from our  $\epsilon_2$  data. Between 0.12 and 4.0 eV,  $N_{\text{eff}}$  was 0.48 electrons per atom for  $\vec{E} \parallel \hat{c}$  and 0.62 electrons per atom for  $\vec{E} \perp \hat{c}$ .

#### ACKNOWLEDGMENTS

The authors wish to thank H. Baker for his advice concerning the electropolishing of the samples and J. Ostenson for performing the residual-resistivity-ratio measurements.

\*Present address: Istituto di Fisica dell'Università, Rome, Italy.

<sup>1</sup>M. P. Givens, Solid State Phys. **6**, 343 (1958).

<sup>2</sup>G. B. Sabine, Phys. Rev. **55**, 1064 (1939).

<sup>3</sup>M. Banning, J. Opt. Soc. Am. **32**, 98 (1942).

<sup>4</sup>G. K. T. Conn and G. K. Eaton, J. Opt. Soc. Am. **44**, 477 (1954).

<sup>5</sup>S. Robin, J. Phys. Radium **14**, 427 (1953).

- <sup>6</sup>J. N. Shklyarevskii and R. G. Yarovaya, *Opt. Spektrosk.* **11**, 661 (1961) [*Opt. Spectrosc.* **11**, 355 (1960)].
- <sup>7</sup>J. Toots, H. A. Fowler, and L. Marton, *Phys. Rev.* **172**, 670 (1968).
- <sup>8</sup>N. Swanson, *J. Opt. Soc. Am.* **54**, 1130 (1964).
- <sup>9</sup>R. E. LaVilla and H. Mendlowitz, *Appl. Opt.* **4**, 955 (1965).
- <sup>10</sup>C. Herring and A. G. Hill, *Phys. Rev.* **58**, 132 (1940).
- <sup>11</sup>J. F. Cornwell, *Proc. R. Soc. A* **A261**, 551 (1961).
- <sup>12</sup>T. L. Loucks and P. H. Cutler, *Phys. Rev.* **133**, A819 (1964).
- <sup>13</sup>J. H. Terrell, *Phys. Rev.* **149**, 526 (1966).
- <sup>14</sup>J. H. Tripp, P. M. Everett, W. L. Gordon, and R. W. Stark, *Phys. Rev.* **180**, 669 (1969).
- <sup>15</sup>J. C. Kimball, R. W. Stark, and F. M. Mueller, *Phys. Rev.* **162**, 600 (1967).
- <sup>16</sup>W. A. Harrison, *Phys. Rev.* **147**, 467 (1966); R. N. Gurzhi and G. P. Motulevich, *Zh. Eksp. Teor. Fiz.* **51**, 1220 (1966) [*Sov. Phys.-JETP* **24**, 1093 (1967)]; A. I. Golovashkin, A. I. Kopeliovich, and G. P. Motulevich, *Zh. Eksp. Teor. Fiz.* **53**, 2053 (1967) [*Sov. Phys.-JETP* **26**, 1161 (1968)].
- <sup>17</sup>D. Brust, *Phys. Rev. B* **2**, 818 (1970).
- <sup>18</sup>N. W. Ashcroft and K. Sturm, *Phys. Rev. B* **3**, 1898 (1971).
- <sup>19</sup>R. V. Kasowski, *Phys. Rev.* **187**, 885 (1969).
- <sup>20</sup>L. W. Bos and D. W. Lynch, *Phys. Rev. B* **2**, 4567 (1970).
- <sup>21</sup>P. A. Jaquet, *Metall. Rev.* **1**, 157 (1956).
- <sup>22</sup>W. C. Walker, D. M. Roessler, and E. Loh, *Phys. Rev. Lett.* **20**, 847 (1968).
- <sup>23</sup>E. Grüneisen and H. K. Adenstedt, *Ann. Phys. (Leipz.)* **31**, 714 (1938); E. Grüneisen and H. D. Erfiling, *Ann. Phys. (Leipz.)* **38**, 399 (1940).
- <sup>24</sup>T. Holstein, *Phys. Rev.* **88**, 1427 (1952); *Phys. Rev.* **96**, 525 (1954).
- <sup>25</sup>R. Fuchs and K. L. Kliewer, *Phys. Rev. B* **2**, 2923 (1970).
- <sup>26</sup>J. F. Cornwell, *Phys. Kondens. Mater.* **4**, 327 (1966).

PHYSICAL REVIEW B

VOLUME 7, NUMBER 8

15 APRIL 1973

## Theory of Metal Surfaces: Induced Surface Charge and Image Potential

N. D. Lang

*IBM Thomas J. Watson Research Center, Yorktown Heights, New York 10598*

W. Kohn\*

*University of California, San Diego, La Jolla, California 92037*

(Received 20 April 1972)

This paper contributes to the theory of the electron density distribution induced at a metal surface by a small static external charge distribution. As a first application, profiles of the charge induced by a uniform external electric field are obtained for metals of different bulk electron densities. A quantity of particular interest is the position of the center of mass,  $x_0$ , of these profiles, for which we present numerical values. (The  $x$  axis is taken along the surface normal.) Next, the case of a small point charge  $q$  with  $x$  coordinate  $x_1$  well outside the surface is treated. It is shown that the image potential experienced by such a charge has the form  $-q^2/[4(x_1 - x_0)]$ , where  $x_0$  is the above-mentioned quantity. We locate  $x_0$ , the effective position of the metal surface, relative to the last lattice plane of the crystal. We discuss the implications of these results for alkali adsorption on metal substrates, the capacitances of small-gap condensers, and field-emission experiments.

### I. INTRODUCTION

In two previous papers<sup>1,2</sup> we have developed a theory of metal surfaces, based on a density-functional formalism.<sup>3,4</sup> We have applied this theory to calculations of the electron charge-density distributions, surface energies, and work functions of metal surfaces. These are all properties of unperturbed surfaces. In the present paper we add a discussion of the screening charges induced in a metal surface by the application of a uniform electric field or by the presence of an external point charge. These induced charges are familiar from elementary electrostatics. However, there they are idealized as being located on a mathematical surface of zero thickness. In reality they are of course spread out, extending over a thickness of the order of  $2 \text{ \AA}$ . The detailed nature of these in-

duced charge densities<sup>5</sup> and its physical implications are the subject of the present paper.

The main contents of the paper are the following.

- (i) We formulate the general linear-response theory.
- (ii) We present the profiles of the additional surface-charge distributions induced by a uniform perpendicular electric field in metals of different bulk electron densities. In particular, we note the positions of the center of mass  $x_0$  of these density distributions, relative to the positive charges, for various bulk electron densities.
- (iii) We show that, to a good approximation, the results of classical elementary electrostatics are valid, provided the idealized mathematical metal surface is taken to pass through  $x_0$ . Thus the image potential for a charge  $q$  located at  $x_1$  is given by